# LOCALIZATION OF THE 3′-TERMINAL END OF THE *Eco*RI B FRAGMENT-SPECIFIC EARLY mRNA OF ADENOVIRUS TYPE 2

Werner BÜTTNER and Zsuzsanna VERES-MOLNAR
*Medizinische Mikrobiologie-Virologie, Ruhr-Universität Bochum, Postfach 102148, 4630 Bochum 1, FRG*

Received 24 October 1980

## 1. Introduction

The early genes of the human adenovirus type 2 (Ad 2), expressed prior to the onset of DNA replication at 6 h post-infection, are involved in regulatory functions necessary for the virus growth cycle and in the oncogenic transformation of mammalian cells. After initial transcription in the nucleus by host cell mechanisms, the early viral RNA species are modified by polyadenylation on the 3′-end, addition of a 5′methyl cap ($m^7$Gppp) and excision of intervening sequences (splicing) to yield mature polysomal mRNA species. The physical map of the early Ad 2 genes reveals 4 separate gene regions, E1–E4, located at the map coordinates 1.5–11 (E1) and 76–86 (E3) on the *r*-strand, and 68–62 (E2) and 99–91.5 (E4) on the *l*-strand (*r* and *l* indicate rightward and leftward transcription of the Ad 2 genome, presented in 100 map units). Each early gene block codes for a family of spliced partially overlapping mRNA species, usually with common 3′-end 5′-termini [1–6]. (Two additional sets of early viral RNA sequences may be present in low copy number, complementary to the map regions 11–14.5 and 20–23.5 on the *l*-strand [7].) The gene product of the region E2 is a DNA-binding protein ($M_r$ 73 000), involved in Ad 2 DNA replication [8,9] and perhaps late gene expression [10]. The characterization of the mRNA of this DNA-binding protein (DBP) is therefore of particular interest. We had calculated the coordinates of the main body of this mRNA by determining the % of radioactivity of DBP mRNA which hybridized to particular subfragments of the *Eco*RI B fragment (map position 58.5–70.7) [11]. Our findings are in good agreement with the data obtained by an $S_1$ nuclease technique [12] and by electron microscopy [6]. We showed that the 3′-terminus of the DBP mRNA lies within the restriction fragment *Bgl*II J (60.2–63.6) at the map position 61.1 ± 0.4. Here, we prepared *Alu*I and *Hpa*II subfragments of *Bgl*II J, and by hybridization to small poly(A)-containing fragments of the DBP mRNA isolated an ~300 basepair subfragment which is homologous to the 3′-terminal region of this mRNA. Analysis of the primary structure of this subfragment identified the DNA sequence which codes for the 3′-terminus of the DBP mRNA.

## 2. Materials and methods

### 2.1. *Restriction endonucleases*

Restriction endonucleases *Eco*RI, *Bgl*II, *Hpa*II, *Alu*I, *Kpn*I, *Hae*III, *Bal*I and *Hha*I [13] were isolated by standard biochemical procedures including ammonium sulfate fractionation, phosphocellulose, DEAE-cellulose and hydroxylapatite chromatography, gel filtration, heparin-agarose and aminoalkyl-agarose affinity chromatography. *Ava*I and *Hph*I were purchased from New England BioLabs.

### 2.2. *DNA restriction fragments*

The preparation of Ad 2 DNA, cleavage with restriction endonucleases and the isolation of the viral DNA fragments from 1.4% agarose gels has been described [3]. Purification of small restriction fragments from polyacrylamide gels was done as in [14].

### 2.3. *φx175 RF I DNA*

RF I DNA of φx174*am*3 was isolated as suggested by W. Rüger, Bochum. *Hae*III fragments of φx174*am*3 [15] were used as DNA $M_r$ markers.

### 2.4. *$^{32}$P-End-labelling of DNA fragments*

Viral DNA fragments were dephosphorylated and end-labelled in the 5′-position with polynucleotide kinase (Boehringer Mannheim) and [$\gamma^{32}$P]ATP [16] as in [14]. A 2–5-fold excess of pmol ATP, spec. act. 1000 Ci/mmol, over pmol 5′-OH ends of DNA was used.

### 2.5. *Size determination of restriction fragments*

$^{32}$P-Labelled fragments were electrophoresed in Hayward's [17] buffer in 140 × 280 × 1.5 mm polyacrylamide slab gels at 100 V for 11 h at 20°C. Covered with Saran wrap, gels were exposed 6–24 h to Kodak X-Omat film at room temperature in the dark. For fragment size analysis, autoradiographs of end-labelled fragments were scanned at 500 nm. Calibration curves between the logarithm of basepairs of $\phi$x174 RF I DNA–*Hae*III fragments and their migration distance were constructed (by linear regression analysis in the linear part of the plot) and used to calculate the molecular weights of unknown fragments.

### 2.6. *Sequence determination*

The sequence was analysed following [14].

### 2.7. *Isolation of poly(A)-containing [$^3$H]RNA fragments*

[$^3$H]Uridine-labelled polysomal RNA was isolated from cycloheximide-treated KB cells 6 h after infection with Ad 2 [18]. Poly(A)-containing RNA was selected [19] by chromatography on poly(U)–Sepharose (Pharmacia Fine Chemicals) according to the supplier's instructions. After ethanol precipitation the RNA was treated with 50 mM $Na_2CO_3$ at 50°C for 20 min as in [20]. This treatment should degrade the *Eco*RI B-specific early mRNA (2400 nucleotides) to RNA fragments 200–250 nucleotides in length. The small poly(A)-containing RNA pieces were recovered by a second poly(U)–Sepharose step and ethanol-precipitated (after addition of 50 $\mu$g/ml carrier tRNA).

### 2.8. *Hybridization of poly(A)-containing RNA pieces to subfragments of* Bgl*II J*

The in vivo [$^3$H]uridine-labelled 3′-terminal RNA fragments were hybridized in 50% formamide [3] to the *Hpa*II and *Alu*I subfragments of *Bgl*II J at 42°C. Filters were washed and treated with 25 $\mu$g/ml pancreatic RNase in 0.3 M NaCl, 0.03 M Na-citrate (2 × SSC), dried and counted in toluene-based scintillator.

## 3. Results and discussion

### 3.1. *Size and map coordinates of the* Hpa*II and* Alu*I subfragments of* Bgl*II J*

Since the available evidence made it most likely that *Bgl*II J (map coordinates 60.2–63.6) is the viral fragment which is homologous to the 3′-terminal region of the early *Eco*RI B-specific mRNA, we decided to cleave *Bgl*II J with two restriction enzymes, *Hpa*II and *Alu*I. The size of the resulting subfragments was determined by electrophoresis in 4% polyacrylamide gels using the *Hae*III fragments of $\phi$x174 RF I DNA as $M_r$ standards. The fragments were endlabelled with [$\gamma^{32}$P]ATP and polynucleotide kinase. Fig.1 shows an autoradiogram of the end-labelled *Bgl*II J subfragments. Lane B depicts the 5 *Alu*I fragment bands of *Bgl*II J (fragments 3 and 4 migrate as a doublet) and lane E shows the 6 *Hpa*II fragments with 4 and 5 as a doublet. For analysis, autoradiographs of end-labelled fragments were scanned and a calibration curve was constructed as in section 2. The calculated

Table 1
Hybridization of poly(A)-containing early viral RNA fragment termini to subfragments of *Eco*RI B

| Subfragment | $^3$H cpm hybridized to Ad 2 DNA equivalents | (%) |
|---|---|---|
| *Eco*RI B/*Bgl*II C | 203 | (0.28) |
| *Bgl*II J | 1465 | (2.01) |
| *Eco*RI B/BglII D | 139 | (0.19) |
| *Bgl*II J/*Hpa*II-1 | 1444 | (1.98) |
| *Bgl*II J/*Hpa*II-2 | 61 | (0.08) |
| *Bgl*II J/*Hpa*II-3 | 31 | (0.04) |
| *Bgl*II J/*Hpa*II-4,5,6 | 47 | (0.06) |
| *Bgl*II J/*Alu*I-1 | 204 | (0.28) |
| *Bgl*II J/*Alu*I-2 | 1181 | (1.62) |
| *Bgl*II J/*Alu*I-3,4 | 207 | (0.28) |
| *Bgl*II J/*Alu*I-5 | 28 | (0.04) |
| *Bgl*II J/*Hpa*II-1/*Alu*I-2 | 1367 | (1.87) |
| *Bgl*II J/*Hpa*II-1/*Alu*I-4 | 117 | (0.16) |
| *Bgl*II J/*Hpa*II-1/*Alu*I-1 | 6 | (0.01) |
| Ad 2 DNA | 42796 | (58.62) |
| Blank filter | 30 | (0.04) |

Ad 2 DNA (10 $\mu$g) and 4 Ad 2 DNA equivalents of each subfragment were used. RNA input was 73 000 $^3$H cpm in 10 $\mu$l hybridization mixture. Background of blank filter is subtracted

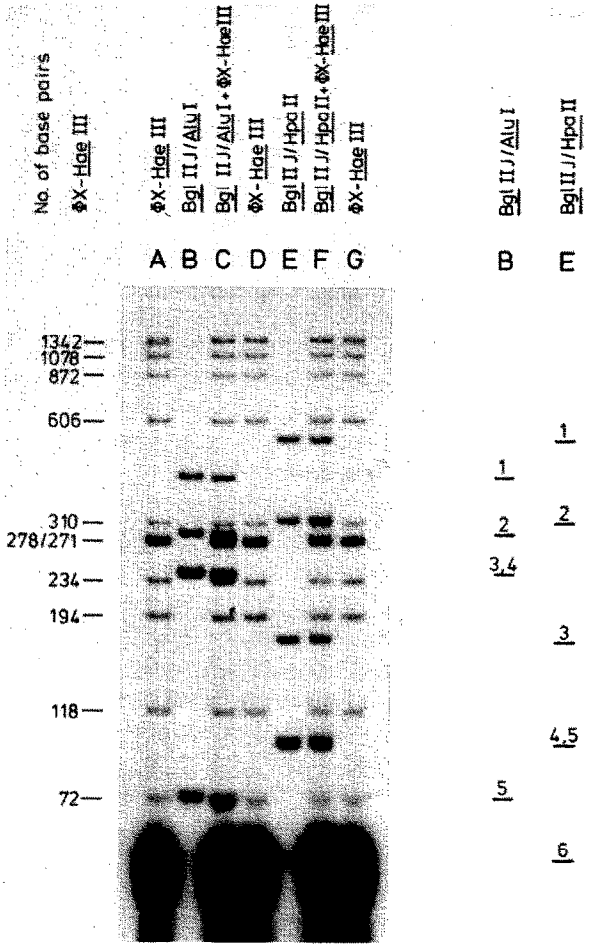


Fig.1. Autoradiogram of $^{32}$P end-labelled *Bgl*II J subfragments. The 11 *Hae*III fragments of φx174 RF I DNA are displayed in lanes A, D and G. Lane B shows the *Alu*I fragments and lane E the *Hpa*II fragments of *Bgl*II J. In lane C and F mixtures of marker DNA and the *Bgl*II J subfragments can be seen. A schematic representation of the fragment bands is given in the right part of the figure.

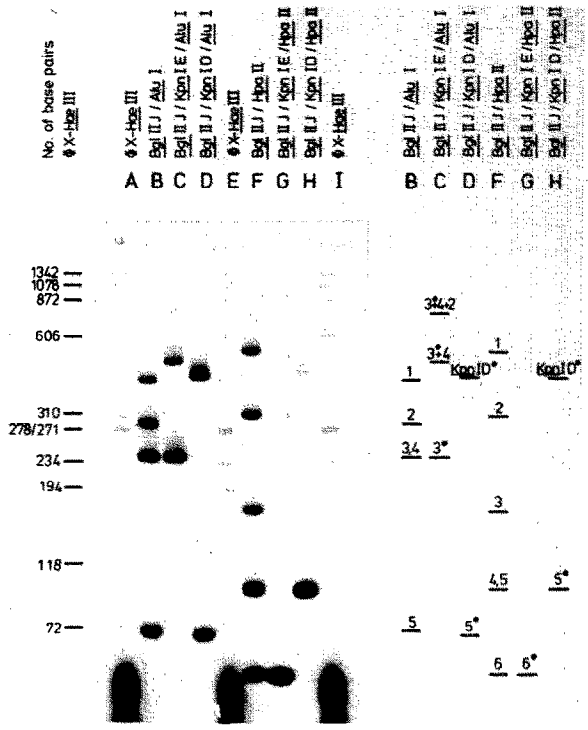


Fig.2. Identification of *Bgl*II J 5′-end fragments. Intact *Bgl*II J was $^{32}$P end-labelled in the 5′ position and restricted once by *Kpn*I at coordinate 61.3. The resulting *Kpn*I fragments *Bgl*II J/*Kpn*I D and *Bgl*II J/*Kpn*I E were cleaved by *Alu*I and *Hpa*II and coelectrophoresed with labelled *Alu*I and *Hpa*II subfragments of *Bgl*II J and the *Hae*III fragments of φx174 RF I DNA. The marker DNA is shown in lanes A, E and I. Lane B shows the 5 *Alu*I subfragments of *Bgl*II J and lane C the *Alu*I subfragments of *Bgl*II J/*Kpn*I E, identifying *Bgl*II J/*Alu*I-3 as end fragment. (In addition lane C reveals the partial *Alu*I digestion products *Bgl*II J/*Alu*I-3 + 4 and *Bgl*II J/*Alu*I-3 + 4 + 2). Lane D depicts the *Alu*I subfragments of *Bgl*II J/*Kpn*I D. Here the end-labelled fragment is identical to *Bgl*II J/*Alu*I-5. The corresponding analysis for the *Hpa*II fragments of 5′-labelled *Bgl*II J is given in lanes F, G and H. The end fragments are *Bgl*II J/*Hpa*II-6 (derived from *Bgl*II J/*Kpn*I E) and *Bgl*II J/*Hpa*II-5 (originating from *Bgl*II J/*Kpn*I D). The right part of fig.2 depicts the scheme of the fragment bands.

$M_r$ values of the *Hpa*II and *Alu*I subfragments of *Bgl*II J are indicated in fig.3.

To position the subfragments we followed the procedure in [21]. *Bgl*II J was end-labelled with [$\gamma^{32}$P]-ATP and polynucleotide kinase. Cleavage with the restriction enzyme *Kpn*I generated 2 singularly 5′-labelled fragments *Bgl*III J/*Kpn*I D (60.2–61.3) and *Bgl*II J/*Kpn*I E (61.3–63.6), which were isolated and further restricted with the enzymes *Alu*I and *Hpa*II. Autoradiograms of complete digests revealed that *Bgl*II J/*Alu*I-3 and *Bgl*II J/*Hpa*II-6 (derived from *Bgl*II J/*Kpn*I E) and *Bgl*II J/*Alu*I-5 and *Bgl*II J/*Hpa*II-5 (originating from *Bgl*II J/*Kpn*I D) were end fragments (fig.2). From partial digests we could deduce the fragment order shown in the cleavage map in fig.3.

### 3.2. *Localization of the 3′-terminal region of the viral RNA of early Ad 2 gene block 2*

To prepare 3′-terminal RNA fragments, poly(A)-containing RNA from [$^3$H]uridine-labelled early polysomal RNA was first degraded by mild alkaline hydrolysis as in section 2. 3′-Terminal RNA fragments were

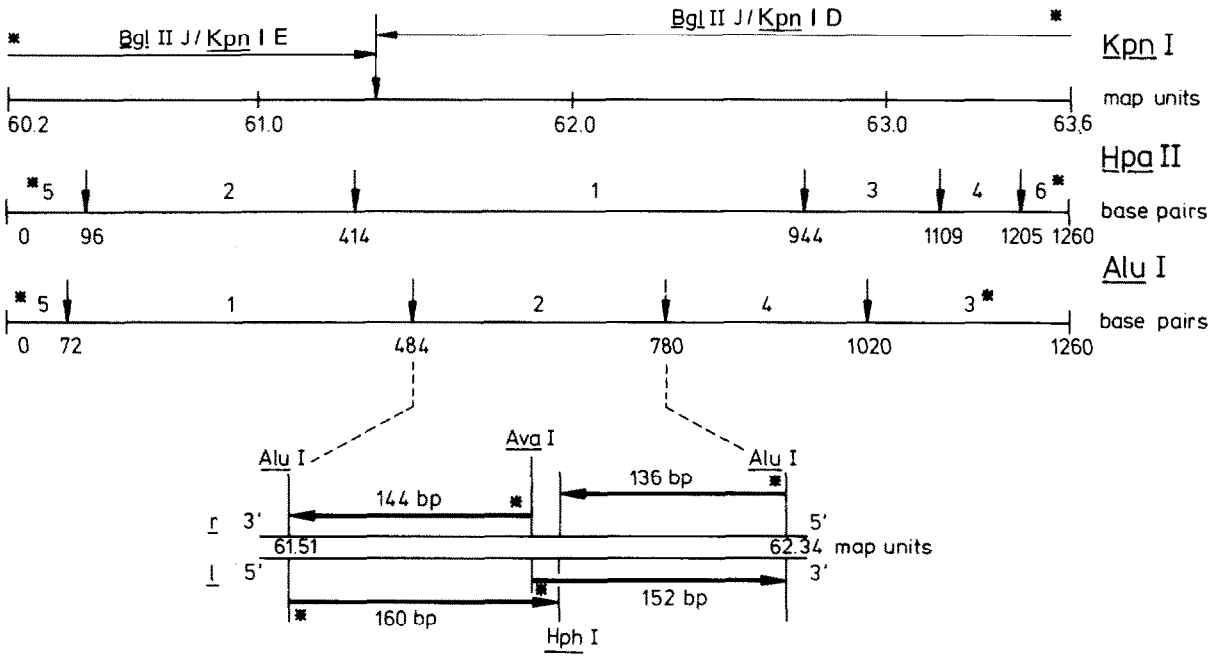


Fig.3. Cleavage map of fragments used for sequence determination of *Bgl*II J/*Alu*I-2. The size and the order of the *Alu*I and *Hpa*II fragments of *Bgl*II J (map coordinates 60.2–63.6, ~1260 basepairs) was determined as in the text. (Two additional *Alu*I sites, 8 and 18 basepairs to the left of the *Alu*I site at 61.51 can be predicted from the DNA sequence of that region; not shown.) *Hph*I and *Ava*I subfragments of *Bgl*II J/*Alu*I-2 (map coordinates 61.51–62.34) were used for sequence determination of both fragment strands (compare lower part of fig.3). *Hph*I cleavage of 5'-labelled *Bgl*II J/*Alu*I-2 yielded a 160 and a 136 basepair fragment, which were isolated and sequenced. The *Ava*I subfragments of *Bgl*II J/*Alu*I-2 (144 and 152 basepairs), used to sequence the opposite strand, were isolated after *Alu*I cleavage of the 5'-labelled *Ava*I subfragments of *Hpa*II-1. (*) Position of the $^{32}$P 5'-label.

```
r 3'  GAAGGACCTCGCGGTGAGCGGGATGAAGGCGTCGGTGTCACGCGTCTAAT   50
l 5'  CTTCCTGGAGCGCCACTCGCCCTACTTCCGCAGCCACAGTGCGCAGATTA

      CCTCGCGGTGAAGAAAAACAGTGAACTTTTTGTACATTTTTATTACATGA  100
      GGAGCGCCACTTCTTTTTGTCACTTGAAAAACATGTAAAAATAATGTACT

      TCCTCTGTGAAAGTTATTTCCGTTTACAAAAATAAACATGTGAGAGCCCA  150
      AGGAGACACTTTCAATAAAGGCAAATGTTTTTATTTGTACACTCTCGGGT

      CTAATAAATGGGGGGTGGGAACGGCAGACGCGGCAAATTTTTAGTTTCCC  200
      GATTATTTACCCCCCACCCTTGCCGTCTGCGCCGTTTAAAAATCAAAGGG

      CAAGACGGCGCGTAGCGATGCGCGGTGACCGTCCCTGTGCAACGCTATGA  250
      GTTCTGCCGCGCATCGCTACGCGCCACTGGCAGGGACACGTTGCGATACT

      CCACAAATCACGAGGTGAATTTGAGTCCGTGTTGGTAGGCGCCGTC  5'  296
      GGTGTTTAGTGCTCCACTTAAACTCAGGCACAACCATCCGCGGCAG  3'
```

Fig.4. Nucleotide sequence of the *Bgl*II J/*Alu*I-2 fragment. The *Bgl*II J/*Alu*I-2 fragment (map coordinates 61.51–62.34) consists of 296 nucleotides. The poly(A) addition signals for the DBP mRNA and the hexon mRNA are indicated by (——) and (– – –), respectively.

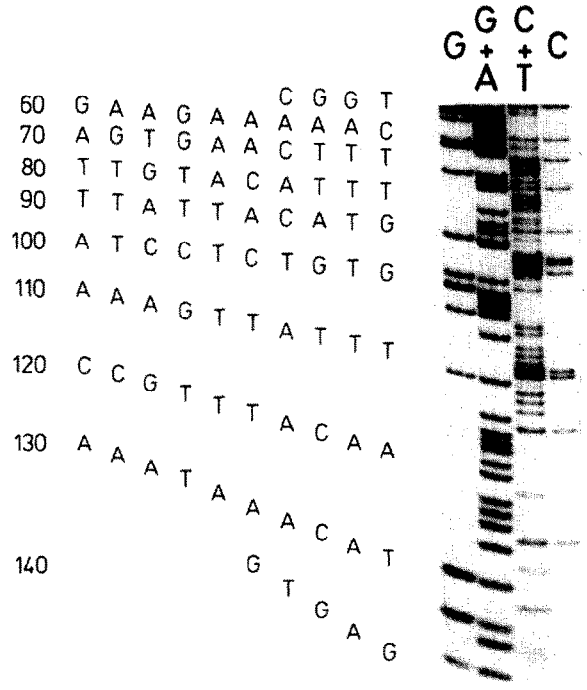


Fig.5. Sequence autoradiograph from the region coding for the 3'-terminus of the DBP and hexon mRNA. The *r*-strand of the 144 basepair long *Ava*I subfragment of *Bgl*II J/*Alu*I-2 is 5'-labelled (fig.3). The polarity of the labelled strand is the same as that of the DBP mRNA and opposite to the hexon mRNA. The poly(A) addition signal for the DBP mRNA can be seen between 130–135 bases from the *Alu*I site at coordinate 61.51, closely preceded by the poly(A) addition signal for the hexon mRNA 114–119 nucleotides from the same *Alu*I site.

subsequently reselected by poly(U)–Sepharose and used for hybridization. To illustrate the yields during the course of this procedure we describe the values of a typical experiment. From 1.7 mg [$^3$H]uridine-labelled early polysomal RNA (spec. act. $1 \times 10^5$ $^3$H cpm/μg), 54.4 μg (3.2%) poly(A)-containing mRNA were selected. $4.9 \times 10^7$ $^3$H cpm (28.8% of the counts in polysomal RNA) were found in this fraction. After alkaline hydrolysis and reselection on poly(U)–Sepharose $3.1 \times 10^6$ $^3$H cpm (6.4% of $^3$H cpm in total poly(A)-positive RNA) were recovered. After ethanol precipitation the 3′-terminal RNA fragments were hybridized in 10 μl aliquots ($7.3 \times 10^4$ $^3$H cpm) to 4 Ad 2 DNA equivalents of the *Bgl*II J subfragments. Table 1 shows that *Bgl*II J/*Hpa*II-1 and *Bgl*II J/*Alu*I-2 hybridize significantly to the 3′-terminal RNA fragments. To confirm these results *Bgl*II J/*Hpa*II-1 was also digested with *Alu*I and used for hybridization (table 1).

### 3.3. *Sequence determination of* Bgl*II J*/Alu*I-2*

To identify the coding region of the 3′-end of the DBP mRNA exactly, we determined the primary structure of the *Bgl*II J/*Alu*I-2 fragment. Our strategy to sequence both strands of this fragment is outlined in the lower part of fig.3. Fig.4 presents the sequence of 296 nucleotides which we confirmed for both strands of *Bgl*II J/*Alu*I-2 (map coordinates 61.51–62.34).

The DBP mRNA is transcribed to the left on the conventional map, thus the *r*-strand has the same polarity as this mRNA. The signal for the poly(A) addition AATAAA [22] close to the 3′-end of the DBP mRNA is present on the *r*-strand 135 nucleotides from the *Alu*I cleavage site at 61.51 m.u. At a distance of 114 nucleotides from the same *Alu*I site very close (10 nucleotides) to the poly(A) addition signal of the DBP mRNA on the *r*-strand, a similar signal on the *l*-strand indicates the 3′-terminal region of the late hexon mRNA, which is transcribed to the right. Fig.5 shows an example of a sequence gel. The *r*-strand was labelled at the *Ava*I cleavage site at map position 61.91, the two poly(A) addition signals for the DBP and the hexon mRNA are shown. Our determination of the genomic localization of the polyadenylation signal of the DBP mRNA by hybridization and DNA sequence analysis places the 3′-terminus of this mRNA at map position 61.89. This agrees very well with the coordinate 61.8 for the 3′-terminus of this mRNA, which was obtained by electron microscopy [6].

**Acknowledgements**

The skillful technical assistance of Jutta Koppe and Barbara Holtmann is gratefully acknowledged. This work was supported by a grant from the Deutsche Forschungsgemeinschaft (Bu 275/2).

**References**

[1] Wold, W. S. M., Green, M. and Büttner, W. (1978) in: Molecular Biology of Animal Viruses (Nayak, D. P. ed) pp. 673–768, Dekker, New York.
[2] Tooze, J. ed. (1980) The Molecular Biology of Tumor Viruses, 2nd edn, Cold Spring Harbor Lab, NY.
[3] Büttner, W., Veres-Molnár, Zs. and Green, M. (1976) J. Mol. Biol. 107, 93–114.
[4] Chow, L. T., Roberts, J. M., Lewis, J. B. and Broker, T. R. (1977) Cell 11, 819–836.
[5] Westphal, H. and Lai, S. (1977) J. Mol. Biol. 116, 525–548.
[6] Chow, L. T., Broker, T. R. and Lewis, J. B. (1979) J. Mol. Biol. 134, 265–303.
[7] Galos, R. S. and Williams, J. (1979) Cell 17, 945–956.
[8] Van der Vliet, P. and Levine, A. (1973) Nature New Biol. 246, 170–174.
[9] Van der Vliet, P., Levine, A., Ensinger, M. and Ginsberg, H. (1975) J. Virol. 15, 348–354.
[10] Klessig, D. F. and Grodzicker, T. (1979) Cell 17, 957–966.
[11] Adamkiewicz, J., Veres-Molnár, Zs. and Büttner, W. (1978) FEBS Lett. 94, 199–203.
[12] Berk, A. J. and Sharp, P. A. (1978) Cell 14, 695–711.
[13] Zabeau, M. and Roberts, R. J. (1979) in: Molecular Genetics (Taylor, J. H. ed) part III, pp. 1–64, Academic Press, London, New York.
[14] Maxam, A. M. and Gilbert, W. (1980) Methods Enzymol. 65, 499–560.
[15] Sanger, F., Air, G. M., Barell, B. G., Brown, N. L., Coulson, A. R., Fiddes, J. C., Hutchinson C. A. iii, Slocombe, P. M. and Smith, M. (1977) Nature 265, 687–695.
[16] Glynn, I. M. and Chappell, J. B. (1964) Biochem. J. 90, 147–149.
[17] Hayward, G. S. (1972) Virology 49, 342–344.
[18] Büttner, W., Veres-Molnár, Zs. and Green, M. (1974) Proc. Natl. Acad. Sci. USA 71, 2951–2955.
[19] Lindberg, U., Person, T. and Philipson, L. (1972) J. Virol. 10, 909–919.
[20] Coffin, J. M. and Billeter, M. A. (1976) J. Mol. Biol. 293–318.
[21] Smith, H. O. and Birnstiel, M. L. (1976) Nucleic Acids Res. 3, 2387–2398.
[22] Proudfoot, N. J. and Brownlee, G. G. (1976) Nature 263, 211–214.